 doi:10.20944/preprints202104.0110.v1

Hydrodechlorination of $CHClF_2$ (HCFC-22) over Pd-Pt catalysts supported on thermally modified activated carbon. Beneficial effect of catalyst oxidation.

Monika Radlik[1,*], Wojciech Juszczyk[2], Wioletta Raróg-Pilecka[3], Magdalena Zybert[3], Zbigniew Karpiński[1,*]

[1] Faculty of Mathematics and Natural Sciences, Cardinal Stefan Wyszyński University in Warsaw, ul. Wóycickiego 1/3, PL-01938 Warszawa, Poland; m.radlik@uksw.edu.pl (M.R.); z.karpinski@uksw.edu.pl (Z.K.)

[2] Institute of Physical Chemistry, Polish Academy of Sciences, ul. Kasprzaka 44/52, PL-01224 Warszawa, Poland; wjuszczyk@ichf.edu.pl (W.J.)

[3] Faculty of Chemistry, Warsaw University of Technology, ul. Noakowskiego 3, PL-00664 Warszawa, Poland; wiola@ch.pw.edu.pl (W.R.-P.); mzybert@ch.pw.edu.pl (M.Z.)

* Correspondence: m.radlik@uksw.edu.pl; z.karpinski@uksw.edu.pl, Tel.: 604 053 267

Abstract: Pd-Pt catalysts supported on carbon preheated to 1600°C have been reinvestigated in $CHFCl_2$ hydrodechlorination. An additionally adopted catalyst oxidation at 350-400°C produced an order of magnitude increase in the catalytic activity of Pd/C. This increase is not caused by changes in metal dispersion or possible decontamination of the Pd surface from superficial carbon, but rather by unlocking the active surface, originally inaccessible in metal particles tightly packed in the pores of carbon. Burning carbon from the pore walls attached to the metal changes the pore structure, providing easier access for the reactants to the entire palladium surface. As upon calcination the performance of the rest of the Pd-Pt/C catalysts changes less than for Pd/C, the relation between the turnover frequency and alloy composition does not confirm the Pd-Pt synergy invoked in our previous work. The use of even higher-preheated carbon (1800°C), completely free of micropores, results in a Pd/C catalyst that does not need to be oxidized to achieve high activity and excellent selectivity up to CH_2F_2 (>90%).

Keywords: hydrodechlorination; $CHClF_2$; Pd-Pt/C; thermally modified carbon; effect of catalyst oxidation; pore structure changes.

1. Introduction

Despite the ban on the use of hydrochlorofluorocarbons (HCFCs) [1], HCFC-22 is still the most abundant HCFC in the atmosphere [2-5]. Massive stocks of HCFC-22 remaining in

Preprints (www.preprints.org) | NOT PEER-REVIEWED | Posted: 5 April 2021 doi:10.20944/preprints202104.0110.v1

refrigeration and air-conditioning systems must be destroyed or, preferably, converted to other valuable chemicals. Catalytic hydrodechlorination appears to be one of most promising technologies for the beneficial utilization of harmful chlorine-containing wastes by transforming them into useful, nontoxic products [6-16]. This strategy was previously proposed for the elimination of dichlorodifluoromethane (CFC-12) by using supported metal catalysts, mainly palladium, where the formation of the environmentally friendly refrigerant HFC-32 (CH_2F_2), was achieved with great selectivities and yields, at relatively low reaction temperatures [6,7,9]. Palladium is also active in $CHClF_2$ hydrodechlorination, showing good product selectivity to the desired CH_2F_2 [6-8,14,15]. However, because of the lower reactivity of this reactant, much higher reaction temperatures must be used than in the case of CCl_2F_2 hydrodechlorination.

Recently, we published results on the hydrodechlorination of $CHClF_2$ over carbon-supported Pd-Pt alloy catalysts [17]. The purpose of selecting a highly preheated (1600°C) commercial Norit carbon was to obtain a catalyst support with a high degree of purity and relatively free of micropores. Bimetallic Pd-Pt/C catalysts, prepared by impregnation, demonstrated better hydrodechlorination activity than the monometallic catalysts, which is consistent with the previous results on hydrodechlorination of other chlorine-containing compounds [9-12,15]. This synergistic effect was attributed to electron charge transfer from platinum to palladium, in line with a generally adopted reaction mechanism of catalytic hydrodechlorination [18] and published data on the electronic structure of Pd-Pt alloys [19].

Although finding the synergy in $CHClF_2$ hydrodechlorination appeared encouraging [17], shortly thereafter we realized that the catalytic activity of carbon-supported palladium was found surprisingly low, at the level of the activity of platinum, regarded as the much less reactive metal in this reaction [15,16]. This raised concerns that the Pd/C catalyst could be partially deactivated. It should be stressed that, during our previous studies, we were well aware of the possibility of blocking the palladium surface by carbon from the support and removing this carbon from the palladium surface. According to suggestions resulting from earlier reports [20], and especially from more recent works [21,22], we pretreated our Pd-Pt/C catalysts with O_2/Ar at 300°C for 1 or 2 h, prior to catalyst activation in H_2 [17]. It should also be noted that our highly preheated turbostratic carbon showed a considerable degree of graphitization [17], resulting in a less serious contamination of the deposited Pd by carbon from the support. As was established in [22], the degree of decoration of the Pd surface by carbon decreases with graphitization of the carbon supports due to stronger C-C interactions.

Preprints (www.preprints.org) | NOT PEER-REVIEWED | Posted: 5 April 2021 doi:10.20944/preprints202104.0110.v1

In this work, we decided to reinvestigate the Pd-Pt/C catalysts more thoroughly. This time, we decided to pretreat our samples at higher than 300°C pre-oxidation temperatures, prior to catalyst reduction. This pretreatment will be referred to as the 'pre-calcination' along the text. Because the pretreatment resulted in a considerable improvement of catalytic performance (especially for Pd/C catalysts), we also performed different tests of catalyst characterization, evaluating for changes in metal dispersion, crystallite size of the metal phase, and changes in the pore structure produced by pre-oxidation. Temperature Programmed Oxidation (TPO) of carbon-supported metal catalysts was intended to provide information on the forms of carbon removed at different stages of catalyst pre-calcination [21].

2. Results

Catalytic screening of both series (ex-acac and ex-chloride) of Pd–Pt/Norit1600 catalysts in $CHClF_2$ hydrodechlorination showed that stable conversions, always <3%, were achieved after a relatively long time-on-stream (~16 h), as reported in our previous paper [17].

Detailed data showing the catalytic properties of Pd-Pt/Norit1600 catalysts pre-calcined at different temperatures are in Tables S1-S4, placed in the Supplementary Materials. The effect of pre-calcination temperature of the catalysts is demonstrated in Figures 1 and 2. As in our previous work [17], for the Pd-rich samples, CH_4 and CH_2F_2 (HFC-32) were found to be the predominant products, making up more than 90% of all products (Tables S1-S4 and Figure 1). For the monometallic Pt samples, CH_3F and CHF_3 made up ~30% of all products. During stabilization, changes in product selectivity were relatively small, and often CH_2F_2 formation was increased at the expense of methane.

The product selectivity presented in Figure 1 (A, B, C) shows the best selectivity to CH_2F_2 for both Pd*100* catalysts (approaching 80%, for reaction temperature ~251°C, Tables S1-S4) and rather smooth changes in the selectivity with addition of platinum. Apart from the parallel, smooth increase in CH_4 selectivity, the catalysts richer in platinum demonstrated the formation of CH_3F and even CHF_3. Regular variations of product selectivity with Pd-Pt alloy composition would imply no synergy in the behavior of the bimetallic system, but rather a linear cumulative effect in the catalytic action of the alloys. These relations resemble very much the previous selectivity patterns obtained for the same catalysts pre-calcined at 300°C for 1 and 2 h [17].

Preprints (www.preprints.org) | NOT PEER-REVIEWED | Posted: 5 April 2021 doi:10.20944/preprints202104.0110.v1

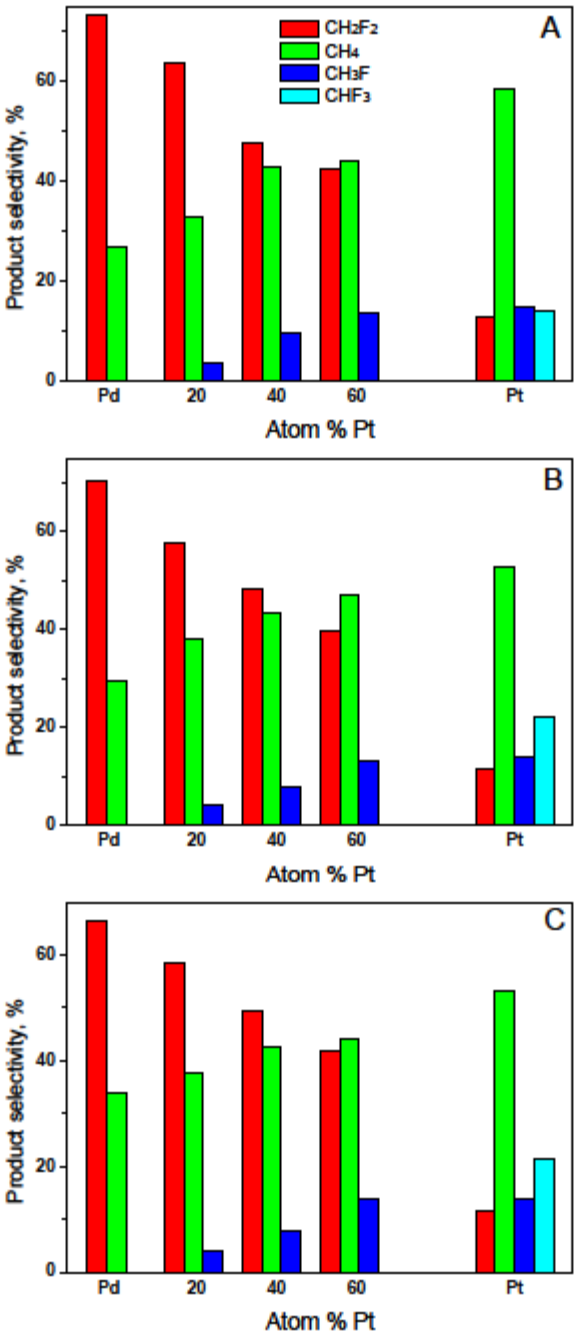

Figure 1. Product selectivity as a function of Pd-Pt alloy composition for the ex-acac series. A – after pre-calcination at 320 ^{o}C (1 h), B - after pre-calcination at 350 ^{o}C (1 h), and C – after pre-calcination at 400 ^{o}C (0.25 h). Reaction temperature 272 ^{o}C. GHSV = 5760 h^{-1}.

Still more interesting results relate to the evolution of catalytic activity of Pd-Pt/Norit1600 systems produced by different pre-calcination conditions. Figure 2 shows that the increase in pre-calcination temperature produces an increase in the activity of all catalysts, however, the Pd-rich catalysts (Pd*100* and Pd*80*Pt*20*) gain the most. The turnover frequency of

Preprints (www.preprints.org) | NOT PEER-REVIEWED | Posted: 5 April 2021 doi:10.20944/preprints202104.0110.v1

Pd100(acac)/Norit1600 experiences a spectacular increase, by nearly an order of magnitude, from ~0.00041 s^{-1} to 0.00263 s^{-1}.

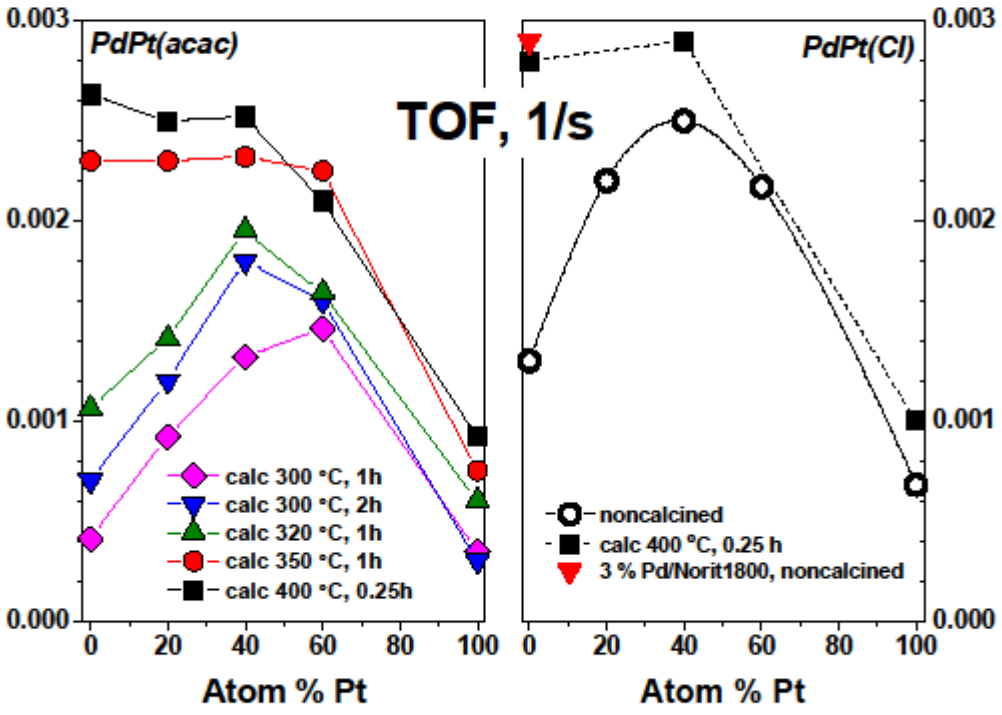

Figure 2. The effect of pre-calcination temperature on catalytic activity (TOF) of Pd-Pt/Norit1600 catalysts vs. nominal Pd-Pt alloy composition. The results for Pd-Pt(acac) catalysts pre-calcined at 300 °C and for Pd-Pt(Cl) non-calcined samples were taken from [17].

Our earlier study [17] showed that the ex-acac Pd-Pt/Norit1600 catalysts were less active than the ex-chloride ones. This is recalled in Figure 2. The reasons for this difference could not be seen rationalized in terms of possible contamination with carbon-containing species because the ex-acac catalysts were subjected to intensive oxidation at 300°C, whereas the ex-chloride samples were not pre-oxidized. Nevertheless, pre-calcination of the ex-chloride samples at 400°C also increases their reactivity (Figure 2). However, a strong maximum for Pd*60*Pd*40* for non-calcined ex-Cl samples is flattened upon pre-calcination. The red triangle in Figure 2 represents the catalytic behavior of 3 wt.% Pd/Norit1800, the catalyst prepared using the Norit carbon preheated in helium at 1800°C [23]. Its basic characteristics is in the Supplementary Materials (Table S4 and SET S1). Its good catalytic performance in $CHClF_2$

Preprints (www.preprints.org) | NOT PEER-REVIEWED | Posted: 5 April 2021 doi:10.20944/preprints202104.0110.v1

hydrodechlorination is achieved without calcination in oxygen. On the other hand, additional calcination practically does not change its catalytic activity (result not shown).

The TOF values have been calculated taking into account the metal dispersions determined by hydrogen chemisorption, H/(Pd+Pt). Metal dispersion did not change significantly with the change in pre-calcination conditions (data in Tables S1-S4 vs. relevant dispersion values reported in [17]). In line with the chemisorption studies, XRD examination of reduced Pd/Norit1600 catalysts confirmed the presence of only minor changes in the metal crystallite size at different pre-calcination temperatures (Figure 3).

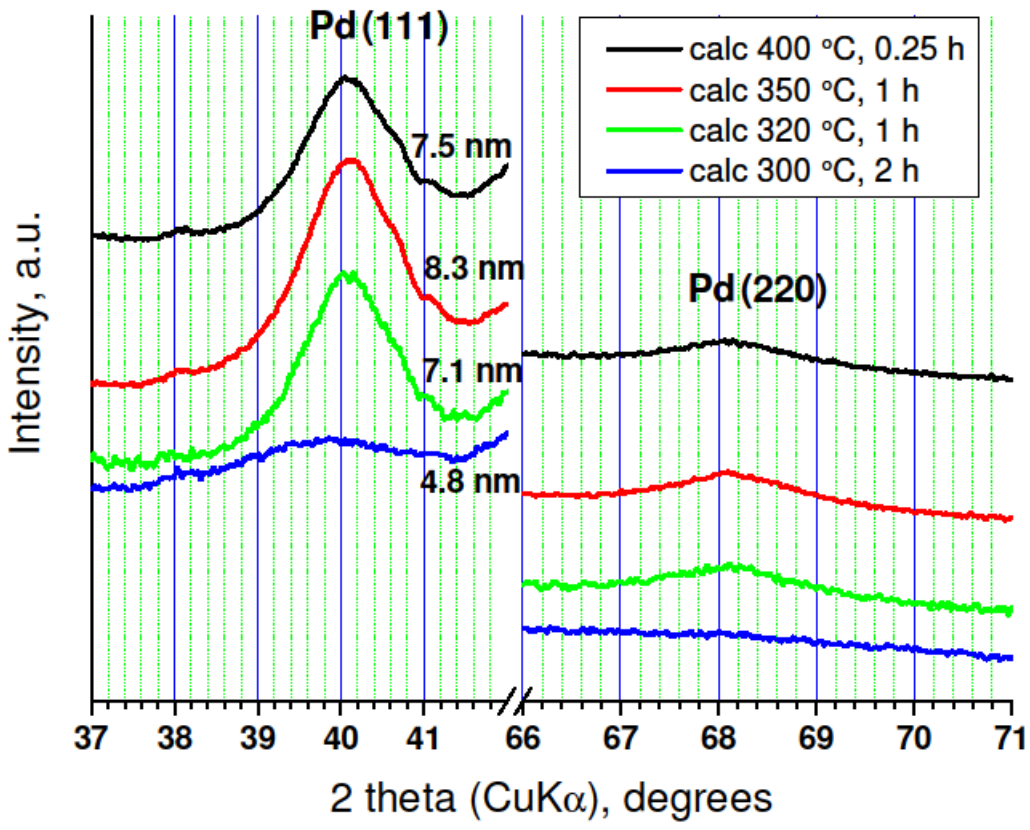

Figure 3. XRD profiles of 2 wt.% Pd/Norit1600 catalysts pre-calcined at different temperatures and reduced at 400 ^{o}C for 1 h.

Thus, if pre-calcination of Pd/Norit1600 does not lead to a significant change in metal dispersion, the large increase in the activity of this catalyst could result from additional cleaning of its surface from carbon. The problem of decorating the surface of palladium with carbon from the carrier has been known for years [20-22]. The relative consistency of the size of the palladium particles resulting from the metal dispersion measurement (d_{Pd} =

Preprints (www.preprints.org) | NOT PEER-REVIEWED | Posted: 5 April 2021 doi:10.20944/preprints202104.0110.v1

1.12/(H/Pd), [24]) and the size of the crystallites Pd (Figure 3) suggests that metal surface decoration does not take place here. It should be added that the pre-treatment of all ex-acac catalysts included their initial pre-calcination at temperatures ≥300°C, a step suggested for carbon elimination from the palladium surface [20-22]. Nevertheless, we decided to carry out TPO measurements of Norit-supported palladium catalysts that could shed light on the forms of carbon eliminated in the course of oxidation.

The results of TGA-TPO studies of the Pd*100*(acac)/C, Pt*100*(acac)/C and Norit1600 carbon are shown in Figure 4. As carbon oxidation (seen as evolution of CO_2) is catalyzed by Pd and Pt, a considerable decrease in the burn-off temperature of carbon, by ~200 ^oC, compared to the oxidation of bare Norit1600 carbon can be observed. However, the shape of TPO profiles for Pd/C and Pt/C does not contain any additional characteristic peaks, which were observed in TPO of Pd/C catalysts by Tengco et al. [21] and could be ascribed to the burn-off of carbon species released from the surface and subsurface layer of palladium. However, our observations are consistent with the results of the cited work because the pre-oxidation of Pd/C at 300°C used in our preliminary catalyst pretreatment appears to be sufficient in order to remove superficial carbon from palladium. Therefore, massive carbon removal (TG) accompanied by vast CO_2 evolution (m/z 44) at temperatures above 300°C (especially at 400°C, see dotted line in Figure 4) should be attributed to the oxidation of support carbon in close contact with metal, called ‘proximate’ carbon in [21].

There are some differences in the course of TPO profiles for both metals. The onset of this increase is for the Pt/C catalyst delayed by ~30°C compared to the behavior of Pd/C (Fig. 4). This 'delay' would be due to the fact that there is less ‘proximate’ carbon near platinum, which, in turn, may be due to the lower adherence of platinum to carbon. It is known that carbon nanotubes are better wetted by palladium than by platinum [25]. However, after exceeding the temperature of ~400°C, platinum shows a higher rate of carbon oxidation. In conclusion, we suggest that the massive firing of pore walls catalyzed by the presence of entrapped metal particles removes steric obstacles for free access of gas reactants to the entire metal surface, making it more active.

Preprints (www.preprints.org) | NOT PEER-REVIEWED | Posted: 5 April 2021 doi:10.20944/preprints202104.0110.v1

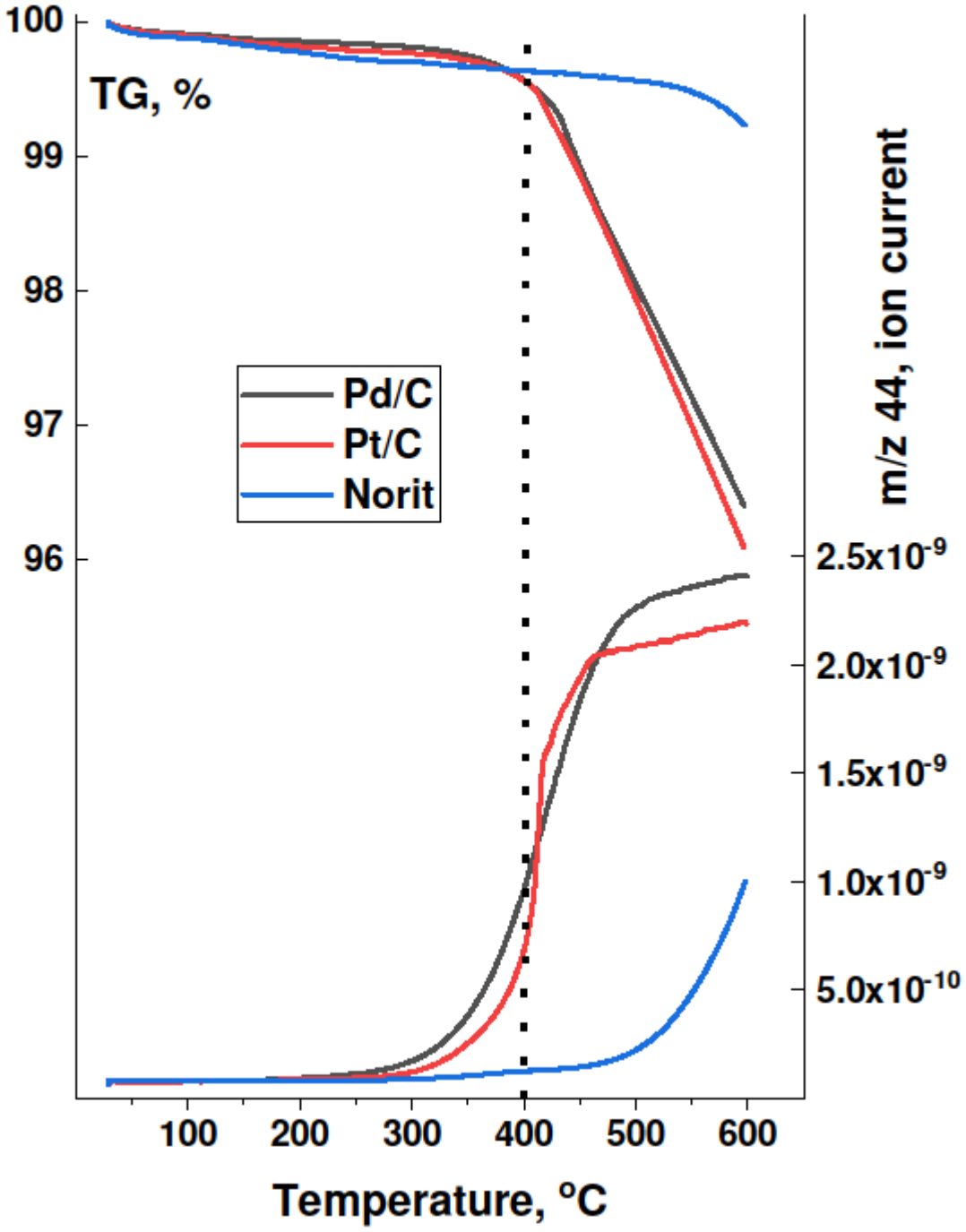

Figure 4. TG-TPO profiles (left axis) of Pd*100*/Norit1600 (black), Pt*100*/Norit 1600 (red) and Norit 1600 carbon (blue). Evolution of CO_2 (right axis) monitored during TGA-TPO at a 5°C/min ramp.

Considerable removal of the 'proximate' carbon at 350-400°C should generate changes in the pore structure of the materials and we decided to check it. The results from the studies of physical adsorption of nitrogen at liquid nitrogen temperatures are presented in Figures 5 and 6, and in Table 1. Figure 5 shows N_2 adsorption isotherms for 2 wt.% Pd/Norit1600, 2 wt.%

Preprints (www.preprints.org) | NOT PEER-REVIEWED | Posted: 5 April 2021 doi:10.20944/preprints202104.0110.v1

Pt/Norit1600 and for unloaded Norit1600. All nitrogen adsorption/desorption isotherms show the hysteresis loop of H3 type, indicating the presence of slit-shaped pores. The figures show trends associated with loading carbon with the metals (impregnation, red lines) and carbon removal by burning (black lines). A relative departure of the red isotherm (for the catalyst) from the blue one (for Norit) is larger for Pd/C than for Pt/C. The results in Table 1 show that the impregnation of Norit1600 with platinum only slightly decreases the BET surface area and pore volume of the system. In the case of palladium, the corresponding changes are larger. This may result from the fact that, on average, the Pt*100*(acac) catalyst contained smaller metal particles than the Pd*100*(acac) (~3 vs. ~7 nm, Table 1 in 17). However, it should be noted that the volume of introduced platinum was ~1.5 times smaller than the volume of introduced palladium (with the same 2 wt. % metal loading in all catalysts).

After oxygen treatment at 400°C, the N_2 adsorption isotherm for Pt/C is more markedly shifted toward higher N_2 uptake than the isotherm for Pd/C. This may result from the higher catalytic activity of platinum (than palladium) in carbon oxidation. Platinum appeared to be a uniquely good metal in soot oxidation [26]. Overall, interesting conclusions follow from the evolution of micropore volume (t_{plot}). Impregnation of Pd leads to a loss of micropore volume by 0.00389 cm^3/g (= 0.00577-0.00188, Table 1). Although the total volume of introduced palladium ~0.0017 cm^3/g would be accommodated in the micropores, it is certain that only a part of Pd nanoparticles blocks the micropores, probably at their outlets. The analysis of the distribution of metal particle size (Table 1 in [17]) indicated the presence of a large variety of differently sized metal particles, some of them would not fit the micropores. Pd/C pre-calcination at 400°C for 15 min recovers a substantial part of micropores, suggesting that very small Pd nanoparticles would now be more accessible to the gas reactants.

Table 1. Surface areas and pore volume data from N_2 adsorption isotherms.

Property		NORIT1600	2 wt.% Pd/NORIT1600		2 wt.% Pt/NORIT1600	
			noncalcined[a]	calcined[b]	noncalcined[a]	calcined[b]
BET surface area, m^2/g		167.8	137.3	192.6	164.1	219.7
BJH pore volume, cm^3/g	from adsorption	0.254	0.229	0.292	0.242	0.286
	from desorption	0.259	0.247	0.302	0.250	0.294
t_{plot} micropore volume, cm^3/g		0.00577	0.00188	0.00335	0.00397	0.00667

[a] After preparation and initial pretreatment (pre-calcined at 300°C, 1 h, not post-calcined at 400°C).

[b] After additional calcination at 400 °C for 0.25 h.

Preprints (www.preprints.org) | NOT PEER-REVIEWED | Posted: 5 April 2021 doi:10.20944/preprints202104.0110.v1

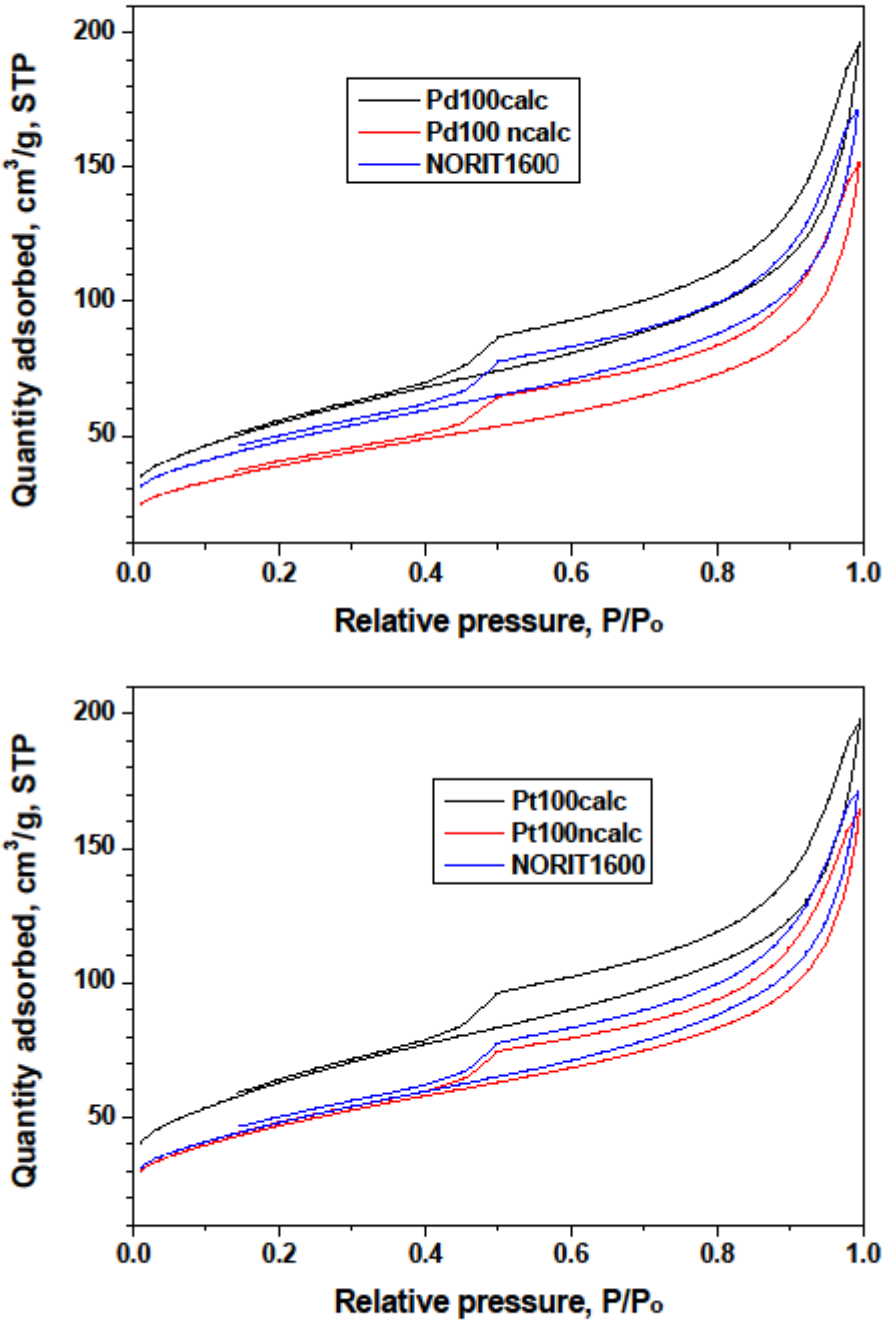

Figure 5. Physical adsorption-desorption isotherms of N_2 on Pd/Norit1600 (top) and Pt/Norit1600 (bottom). The isotherm for Norit1600is included in the graphs.

Figure 6 presents variations in the pore size distribution in impregnated and calcined Norit1600, Pd/C and Pt/C catalysts. Again, the pore structure of the Pt*100*/C catalyst does not differ much from the structure of Norit1600 (black vs. white bars in Figure 6). For Pd100, the differences are larger: all black bars (with exception for very large pores) are smaller than the

Preprints (www.preprints.org) | NOT PEER-REVIEWED | Posted: 5 April 2021 doi:10.20944/preprints202104.0110.v1

white ones. This would indicate a widespread distribution of Pd particles over Norit1600, i.e., the metal location throughout the entire pore structure. On the other hand, the calcination of these catalysts leads to a roughly uniform volume increase in all pores, regardless of their size. Earlier studies [27] on graphite oxidation by Pd and Pt showed that all active metal particles, irrespective of their size, gasify the same amount of carbon per unit time under given experimental conditions. In the case of Pt*100*, a somewhat higher increase in the volume of small pores with 2.2-2.8 nm diameter can be observed. This pore size corresponds with the mean size of metal particles in the reduced Pt*100*(acac) catalyst.

Preprints (www.preprints.org) | NOT PEER-REVIEWED | Posted: 5 April 2021 doi:10.20944/preprints202104.0110.v1

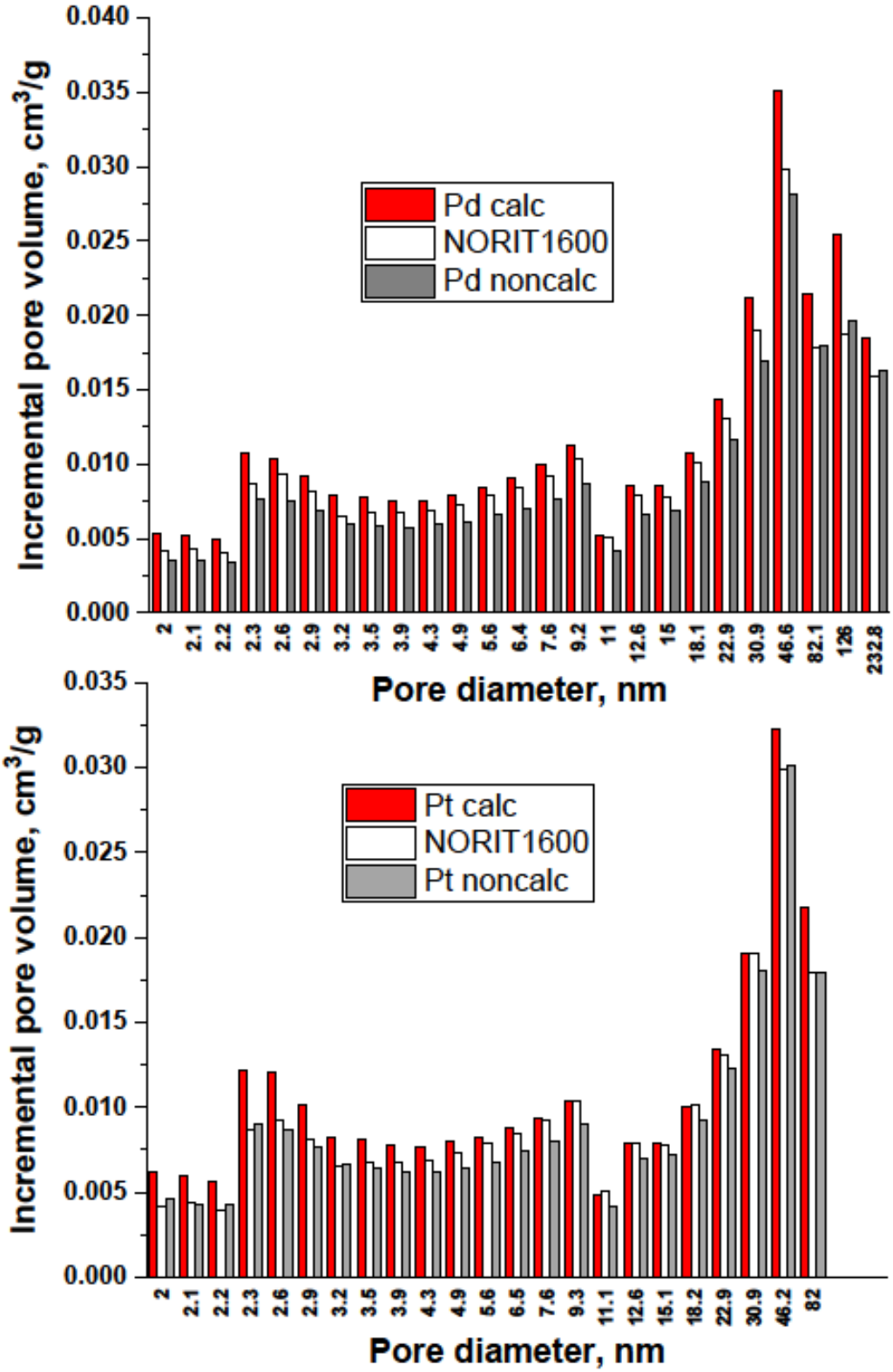

Figure 6. Pore size distribution of differently pretreated Pd/Norit1600 (top) and Pt/Norit1600 (bottom) catalysts.

Preprints (www.preprints.org) | NOT PEER-REVIEWED | Posted: 5 April 2021 doi:10.20944/preprints202104.0110.v1

From the results of the physical characterization of Norit1600 supported Pd and Pt catalysts, one can conclude:

1) Oxidation of Pd-on-highly preheated Norit catalyst, which leads to nearly an order of magnitude increase in catalytic activity cannot be the result of marked changes in metal dispersion changes because such changes have not been found.

2) Possible decontamination of palladium surface from carbon by oxidation at 350-400°C is also rejected as a basic reason for the activity increase. Preliminary pre-calcination of Pd/Norit1600 samples at 300°C for 1-2 h should remove the carbon from the metal surface [21,22]. TPO profiles of such catalysts do not contain any signs of presence of such carbon species.

3) TGA-MS studies show the beginning of a massive removal of a "proximate" carbon at the temperature 350°C. Metal-catalyzed burning of carbon support changes the pore structure of Norit1600. In particular, the micropore volume is vastly increased along with catalyst oxidation. Metal nanoparticles, wetting small pores of the support, presumably lose contact with the pore walls as a result of oxidation. Such a catalyst represents enhanced reactivity, proving the accessibility of the active sites to reactants.

Figure 2 showed the effect of calcination temperature on the catalytic performance in $CHClF_2$ hydrodechlorination. By increasing the activity of Pd and Pd-rich alloys as an effect of an increased temperature of calcination, the relation between TOF and PdPt alloy composition changes its primary course. The Pd-Pt/C samples pre-calcined at 300 and 320°C show the sharp maximum at 40 at.% Pt, but after pre-calcination at ≥350°C, this maximum disappears. This means that the synergistic effect in catalytic action of Pd and Pt reported in our previous paper [17] ceases to exist. The previously discussed product selectivity data are also in opposition to the synergy. Figure 7 summarizes the results of our previous and present study. The course of the relation between the TOF and Pd-Pt alloy concentration after burning carbon from pore walls does not contain any maxima but tends to reflect the inferred Pd content in the surface layer of Pd-Pt alloys (inset in Figure 7). This suggests that the course of $CHClF_2$ hydrodechlorination on Pd-Pt surfaces would be controlled by the presence of Pd on the surface, with active sites composed of single Pd atoms.

Preprints (www.preprints.org) | NOT PEER-REVIEWED | Posted: 5 April 2021 doi:10.20944/preprints202104.0110.v1

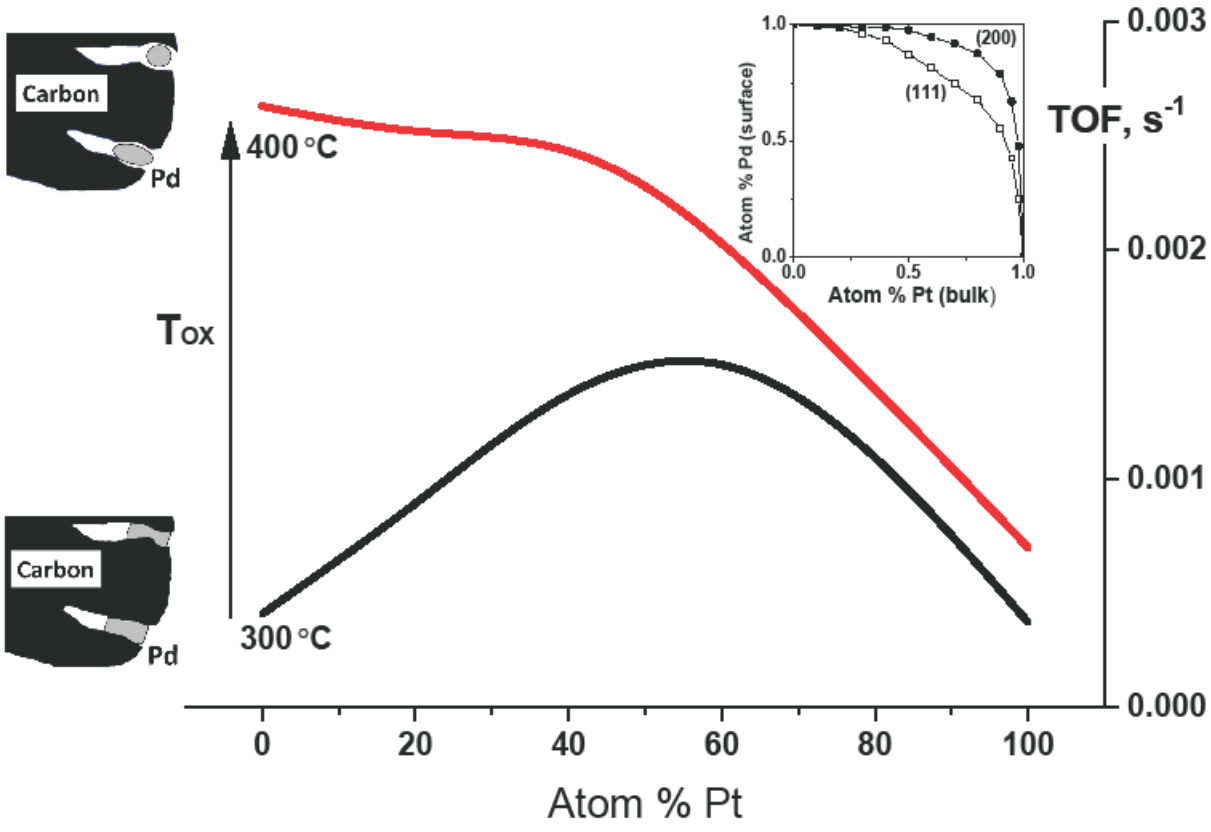

Figure 7. Changes in the catalytic behavior of Pd-Pt/C catalysts in $CHClF_2$ hydrodechlorination caused by catalyst pre-calcination. Inset: the relation between surface and bulk composition of Pd–Pt alloys adapted from Rousset et al. [28].

Good catalytic performance of non-calcined 3 wt.% Pd/Norit1800 catalyst used in our earlier work [23], shown in Figure 2 (red triangle), should be commented on. A relatively low BET surface area and pore size distribution in this sample (SET S1 in Supplementary Materials) appear to favor good access of reactants to active sites. The very small micropore volume in this impregnated catalyst (0.0010 cm^3/g, SET S1), in combination with the lack of micropores in carbons heated at 1800°C [29], confirms the absence of Pd particles in micropores.

We decided to investigate the 3 wt.% Pd/Norit1800 catalyst in $CHClF_2$ hydrodechlorination using somewhat intensified reaction conditions, i.e., relatively low GHSV values. Figure 8 shows good stability and very good selectivity to CH_2F_2 (90-95%). This result calls for further studies with use of very highly pretreated carbons.

Preprints (www.preprints.org) | NOT PEER-REVIEWED | Posted: 5 April 2021 doi:10.20944/preprints202104.0110.v1

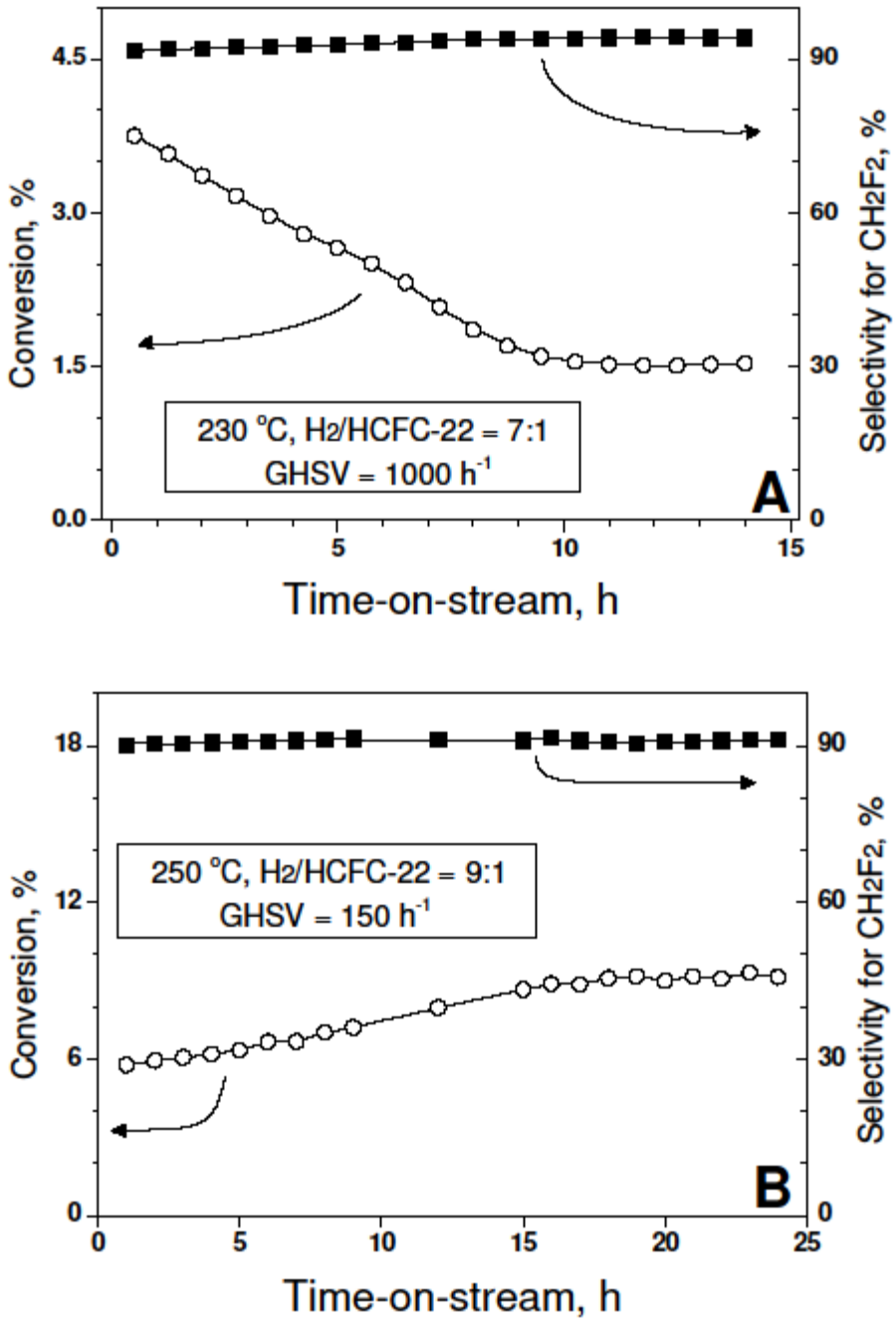

Figure 8. Time-on-stream behavior (conversion of $CHClF_2$ and selectivity to CH_2F_2) of 3 wt. % Pd/carbon. Norit RO 08 carbon support was heated in helium at 1800 °C for 2 h. Reaction conditions are included in figure frames.

3. Methods

3.1. Catalyst Preparation

The preparation and basic pretreatment were described in our previous paper [17]. Briefly, Norit RO 0.8 activated carbon, pretreated in helium at 1600°C for 2 h (referred in the text as

Preprints (www.preprints.org) | NOT PEER-REVIEWED | Posted: 5 April 2021 doi:10.20944/preprints202104.0110.v1

Norit1600), was co-impregnated with a toluene solution of the metal acetylacetonates, to prepare monometallic Pd and Pt and three bimetallic Pd-Pt catalysts (atomic ratio of Pd-to-Pt: 80:20, 60:40 and 20:80), designed as Pd*X*Pt*Y*, where *X* and *Y* stand for atomic percentages of Pd and Pt in the metal phase. The overall metal loading was 2 wt.%.

As mentioned in the previous report [17], the removal of the organic part of acetylacetonates achieved by calcination in flowing 1% O_2/Ar (50 cm^3/min, at STP) at 300°C for 1 h. In our previous work, the pre-calcined catalysts were subjected to reduction in the flow of the H_2/Ar mixture (20 cm^3/min, STP) at 400°C before the reaction. In the present work, the stored catalysts were subjected to more severe secondary calcinations in O_2/Ar at 320°C, 350° and 400°C.

Some kinetic runs were performed with a few Pd, Pt and Pd-Pt catalysts prepared from the chloride precursors. Their preparation was also described in [17].

3.2. *Catalytic Tests*

The hydrodechlorination of chlorodifluoromethane was conducted in a glass flow system equipped with a gradientless reactor, as described previously [17]. Prior to each reaction run, the catalyst (0.20 g sample) was subjected to pre-calcination step in flowing 1% O_2/Ar (20 cm^3/min, STP) at 320°C and 350°C for 1 h, or at 400 °C for 15 min. The pre-calcination was followed by a short purge with Ar at 400°C, and the reduction in 10% H_2/Ar (20 cm^3/min, STP) at 400°C for 1 h. After reduction, the catalysts were cooled in H_2/Ar flow to the desired initial reaction temperature, i.e., 270°C. For a typical reaction run, the total flow of the reactant mixture was 48 cm^3/min and consisted of $CHClF_2$ (1 cm^3 /min), H_2 (8 cm^3/min) and Ar (39 cm^3/min), fixing the GHSV at 5760 h^{-1}. This high value allowed the maintenance of low conversions, usually <3%, and minimized secondary reactions. The reaction was carried out until a steady state was achieved at 270°C (~16 h). Then, the reaction temperature was gradually decreased to 260°C and 250°C and new experimental points were collected. A typical run lasted ~20 h. The post-reaction gas was analyzed by gas chromatography. Some kinetic runs were performed with a few pre-calcined Pd-Pt/C catalysts prepared from metal chlorides. In those cases, the reduction in H_2/Ar at 400°C lasted 3 h. Finally, the 3 wt.% Pd supported on Norit carbon preheated at 1800°C, used in our previous studies [23], was also tested.

3.3. *Catalyst Characterization by H_2 Chemisorption, XRD, Temperature Programmed Oxidation, and Physical Adsorption (BET, pore structure)*

Preprints (www.preprints.org) | NOT PEER-REVIEWED | Posted: 5 April 2021 doi:10.20944/preprints202104.0110.v1

As in our previous work [17], metal (Pd, Pt) dispersion was determined using hydrogen chemisorption, following the procedure recommended by Bartholomew for Fe, Co and Ni catalysts [30]. A reduced and outgassed catalyst was saturated with hydrogen at 70°C, and the amount of adsorbed hydrogen was measured through temperature programmed desorption in an argon stream, increasing the temperature 20°C/min.

XRD (X-Ray Diffraction) studies of reduced and, in a few cases, post-reaction samples of Pd-Pt/C catalysts were performed on a standard Rigaku–Denki diffractometer using Ni-filtered Cu$K\alpha$ radiation. The samples were scanned using a step-by-step technique, at 2θ intervals of 0.05° and a recording time of 10 s for each step.

Thermogravimetric analysis coupled with mass spectrometry (TGA-MS) was carried out using the flow system of the STA449C thermobalance (NETZSCH) with the QMS 403C Aeolos quadrupole mass spectrometer (NETZSCH). Measurements were conducted on the samples of Norit1600, Pd*100*(acac)/C and Pt*100*(acac)/C of ~35 mg each, which were heated at a constant rate of 5°C/min in the temperature range of 30-600°C, under a 1% O_2/Ar mixture flow (100 cm^3/min, at STP). The temperature, mass changes and mass signals of selected gases (O_2, CO, CO_2, H_2O) were continuously recorded during these TPO measurements.

Surface areas and porosities were measured with an ASAP 2020 instrument from Micromeritics, employing the BET (Brunauer–Emmett–Teller), t-Plot, BJH (Barrett–Joyner–Halenda) and HK (Horvath–Kawazoe) methods and using nitrogen as the adsorbate. Before measuring the adsorption isotherm at 77 K, the sample was kept at 200°C for 5 h in a vacuum to clean its surface.

4. Conclusions

Two series of Pd-Pt catalysts (ex-metal acetylacetonates and ex-metal chlorides) supported on Norit activated carbon preheated at 1600°C have been reinvestigated in the hydrodechlorination of chlorodifluoromethane. An additionally adopted catalyst oxidation pretreatment, at 320, 350 and 400°C, resulted in an order of magnitude increase in catalytic activity of the monometallic Pd/C. Neither possible changes in metal dispersion nor metal decontamination from carbon were found responsible for this effect. TGA-MS studies show the beginning of massive removal of a “proximate” carbon at the temperature 350°C, i.e., at the onset of the increase in catalytic activity. Metal-catalyzed burning of carbon support modifies the pore structure of Norit1600. The micropore volume in particular is vastly increased as an effect of catalyst oxidation. Metal nanoparticles, wetting the small pores of the support, presumably lose contact with the pore walls as a result of oxidation. Such a catalyst

demonstrates enhanced reactivity, hence proving the accessibility of the active sites to reactants. Therefore, the reactivity tuning of Pd/C catalysts using oxidation is not due to changes in metal dispersion but from unlocking the active metal surface, originally inaccessible in Pd particles tightly packed in the pores of carbon. In agreement with our speculations, a non-calcined Pd/C catalyst supported on the carbon preheated at 1800°C showed good catalytic behavior. Separate runs with 3 wt.% Pd/carbon under somewhat intensified reaction conditions presented very good catalyst stability and excellent selectivity to CH_2F_2 (>90%).

In our discussion we did not consider the possible inhibiting role of residual chloride originating from the metal precursor for two reasons. First, the ex-chloride catalysts were generally more active than the ex-acac ones. Second, during the reaction of $CHClF_2$ hydrodechlorination, the metal surface, regardless of its origin, is covered by a variety of active Cl/F and HCl/HF species, so the possible role of residual chloride from the precursor would be difficult to distinguish.

Supplementary Materials:

Table S1: $CHClF_2$ hydrodechlorination on Pd-Pt/(acac)/Norit1600 catalysts precalcined at 320 ^oC for 1 h. Turnover frequencies, product selectivities and activation energies, Table S2: $CHClF_2$ hydrodechlorination on Pd-Pt/(acac)/Norit1600 catalysts precalcined at 350 ^oC for 1 h. Turnover frequencies, product selectivities and activation energies, Table S3: $CHClF_2$ hydrodechlorination on Pd-Pt/(acac)(/Nortit1600 catalysts precalcined at 400 ^oC for 15 min. Turnover frequencies, product selectivities and activation energies, Table S4: $CHClF_2$ hydrodechlorination on Pd-Pt/Norit catalysts prepared from metal chlorides. Turnover frequencies, product selectivities and activation energies, SET S1. Characteristic of 3 wt.% Pd/Norit1800 catalyst.

Author Contributions: M.R. was responsible for conceptual work, catalysts synthesis and characterization by chemisorption, kinetic studies, experiment planning and manuscript writing; W.J. was responsible for catalyst characterization by XRD; W.R.-P. and M.Z. were responsible for preparation and characterization of catalyst support; Z.K. was responsible for conceptual work, experiment planning and overall care about manuscript writing.
All authors have read and agreed to the published version of the manuscript.

Funding: This work was carried out within Research Project # 2016/21/B/ST4/03686 from the National Science Centre (NCN), Poland.

Conflicts of Interest: The authors declare no conflict of interest.

References

1. Chlorodifluoromethane, ttps://en.wikipedia.org/wiki/Chlorodifluoromethane.
2. Montzka, S.A.; McFarland, M.; Andersen, S.O.; Miller, B.R.; Fahey, D.W.; Hall, B. D.; Hu, L.; Siso, C.; Elkins, J. W. Recent trends in global emissions of hydrochlorofluorocarbons and hydrofluorocarbons: Reflecting on the 2007 Adjustments to the Montreal Protocol. J. Phys. Chem. A 2015, 119, 4439-4449.
3. Montzka, S.A.; Dutton, G.S.; Yu, P.; Ray, E.; Portmann, R.W.; Daniel, J.S.; Kuijpers, L.; Hall, B.D.; Mondeel, D.; Siso, C.; Nance, J.D.; Rigby, M.; Manning, A.J.; Hu, L.; Moore, F.; Miller, B.R.; Elkins, J.W. An unexpected and persistent increase in global emissions of ozone-depleting CFC-11. Nature 2018, 557, 413-417.
4. Prignon, M.; Chabrillat, S.; Minganti, D.; O'Doherty, S.; Servais, Ch.; Stiller, G.; Toon, G.C.; Vollmer, M.K.; Mahieu, E. Improved FTIR retrieval strategy for HCFC-22 (CHClF2), comparisons with in situ and satellite datasets with the support of models, and determination of its long-term trend above Jungfraujoch. Atmos. Chem. Phys. 2019, 19, 12309-12324.
5. Oram, D.E.; Ashfold, M.J.; Laube, J.C.; Gooch, J.L.; Humphrey, S.; Sturges, W.T.; Leedham-Elvidge, E.; Forster, G.L.; Harris, N.R.P.; Iqbal Mead, M.; Abu Samah, A.; Phang, S.M.; Ou-Yang, Ch.-F.; Lin, N.-H.; Wang, J.-L.; Baker, A.K.; Brenninkmeijer, C.A.M.; Sherry, D. A growing threat to the ozone layer from short-lived anthropogenic chlorocarbons. Atmos. Chem. Phys. 2017, 17, 11929-11941.
6. Morato, A.; Alonso, C.; Medina, F.; Cesteros, Y.; Salagre, P.; Sueiras, J.E.; Tichit, D.; Coq, B. Palladium hydrotalcites as precursors for the catalytic hydroconversion of CCl_2F_2 (CFC-12) and $CHClF_2$ (HCFC-22). *Appl. Catal. B* **2001**, *32*, 167-179.
7. Morato A.; Medina, F.; Sueiras, J.E.; Cesteros, Y.; Salagre, P.; de Menorval, L. C.; Tichit, D.; Coq, B. Characterization and catalytic properties of several $KMg_{1-x}Pd_xF_3$ with perovskite-like structures for the hydroconversion of $CHClF_2$. *Appl. Catal. B* 42 (2003) 251-264.
8. Yu, H.; Kennedy, E.M.; Uddin, Md. A.; Sakata, Y.; Dlugogorski, B.Z. Gas-phase and Pd-catalyzed hydrodehalogenation of $CBrClF_2$, CCl_2F_2, $CHClF_2$, and CH_2F_2. *Ind. Eng. Chem. Res.* **2005**, *44*, 3442-3452.
9. Legawiec-Jarzyna, M.; Śrębowata, A.; Juszczyk, W.; Karpiński, Z. Hydrodechlorination over Pd-Pt/Al_2O_3 catalysts A comparative study of chlorine removal from

dichlorodifluoromethane, carbon tetrachloride and 1,2-dichloroethane. *Appl. Catal. A* **2004,** *271*, 61-68.

10. Martin-Martinez, M.; Gómez-Sainero, L.M.; Bedia, J.; Arevalo-Bastante, A.; Rodriguez., J.J. Enhanced activity of carbon-supported Pd-Pt catalysts in the hydrodechlorination of dichloromethane. *Appl. Catal. B* **2016,** *184*, 55-63.
11. Bedia, J.; Gómez-Sainero, L.M.; Grau, J.M.; Busto, M.; Martin-Martinez, M.; Rodriguez, J.J. Hydrodechlorination of dichloromethane with mono- and bimetallic Pd-Pt on sulfated and tungstated zirconia catalysts. *J. Catal*. **2012,** *294*, 207-215.
12. Garcia, C.M.; Woolfolk, L.G.; N. Martin, N.; Granados, A.; de los Reyes, J.A. Evaluation of mono and bimetallic catalysts supported on Al_2O_3-TiO_2 in the reaction of hydrodechlorination of 1,2-dichloroethane. *Rev. Mex. Ing. Quim*. **2012,** *11*, 463-468.
13. Han, W.; Li, X.; B. Liu, B.; L. Li, L.; Tang, H.; Li, Y.; Ch. Lu, CH.; X. Li, X. Microwave assisted combustion of phytic acid for the preparation of Ni2P@C as a robust catalyst for hydrodechlorination. *Chem. Commun*. **2019**, *55*, 9279-9282.
14. Schoebrechts, J.-P.; Doiceau, G.; Wilmet, V. Catalytic system comprising a hydrogenation catalyst on a support and process for the hydrodechlorination of chlorofluorinated hydrocarbons. US Patent 5561069 (1996), to Solvay.
15. Martin-Martinez, M.; Gómez-Sainero, L.M.; Palomar, J.; Omar, S.; Rodriguez, J.J. Dechlorination of dichloromethane by hydrotreatment with bimetallic Pd-Pt/C catalyst. *Catal. Lett*. **2016,** *146*, 2614-2621.
16. Patil, P.T.; Dimitrov, A.; Kirmse, H.; Neumann, W.; Kemnitz, E. Non-aqueous sol–gel synthesis, characterization and catalytic properties of metal fluoride supported palladium nanoparticles. *Appl. Catal. B* **2008,** *78*, 80-91.
17. Radlik, M.; Juszczyk, W.; Matus, K.; Raróg-Pilecka, W.; Karpiński, Z. Hydrodechlorination of $CHClF_2$ (HCFC-22) over Pd–Pt catalysts supported on thermally modified activated carbon. *Catalysts* **2020**, *10*, 1291.
18. Chen, N.; Rioux, R.M.; Barbosa, L.A.M.M.; Ribeiro, F.H. Kinetic and theoretical study of the hydrodechlorination of $CH_{4-x}Cl_x$ (x = 1-4) compounds on palladium. *Langmuir* **2010,** *26*, 16615–16624.
19. Rosantha Kumara, L.S.R.; Sakata, O.; Kobayashi, H.; Song, C.; Kohara, S.; Ina, T.; Yoshimoto, T.; Yoshioka, S.; Matsumura, S.; Kitagawa, H. Hydrogen storage and stability properties of Pd–Pt solid-solution nanoparticles revealed via atomic and electronic structure. *Sci. Rep*. 7 (2017) article 14606; doi:10.1038/s41598-017-14494-7).

20. Krishnankutty, N.; Li, J.; Vannice, M.A. The effect of Pd precursor and pretreatment on the adsorption and absorption behavior of supported Pd catalysts. *Appl. Catal. A* **1998**, *173*,137-144.
21. Tengco, J.M.M.; Lugo-José, Y.K.; Monnier, J.R.; Regalbuto, J.R. Chemisorption–XRD particle size discrepancy of carbon supported palladium: Carbon decoration of Pd? *Catal. Today* **2015**, *246*, 9-14.
22. Banerjee, R.; Regalbuto, J.R. Rectifying the chemisorption – XRD discrepancy of carbon supported Pd: Residual chloride and/or carbon decoration. *Appl. Catal. A* **2020**, *595*, 117504.
23. Bonarowska M.; Burda, B.; Juszczyk, W.; Pielaszek, J.; Z. Kowalczyk, Z.; Karpiński, Z. Hydrodechlorination of CCl_2F_2 (CFC-12) over Pd-Au/C catalysts, *Appl. Catal. B* **2001**, *35*, 13-20.
24. Ichikawa, S.; Poppa, H.; Boudart, M. Disproportionation of CO on small particles of silica-supported palladium. *J. Catal*. **1985**, *91*, 1-10.
25. Lee, S.; S.-J. Kahng, S.-J.; Kuk, Y. Nano-level wettings of platinum and palladium on single-walled carbon nanotubes. *Chem. Phys. Lett.* **2010**, *500*, 82-85.
26. Uchisawa J.O.; Obuchi, A.; Zhao, Z.; Kushiyama, S. Carbon oxidation with platinum supported catalysts. *Appl. Catal. B* **1998**, *18*, L183-L187.
27. Baker, R.T.K.; France, J.A.; Rouse, L.; Waite, R.J. Catalytic oxidation of graphite by platinum and palladium. *J. Catal*. **1976**, *41*, 22-29.
28. Rousset, J.L.; Bertolini, J.C.; Miegge, P. Theory of segregation using the equivalent-medium approximation and bond-strength modifications at surfaces: application to fcc Pd-X alloys. *Phys. Rev. B* **1996**, *53*, 4947–4957.
29. Zheng, X.; Zhang, S.; Xu, J.; We, K. Effect of thermal and oxidative treatments of activated carbon on its surface structure and suitability as a support for barium promoted ruthenium in ammonia synthesis catalysts. *Carbon* **2002**, *40*, 2597–2603.
30. Bartholomew, C.A. Hydrogen adsorption on supported cobalt, iron and nickel. *Catal. Lett.* **1990**, *7*, 27-52.